JOURNAL OF MATERIALS SCIENCE 19 (1984) 1089–1098

Nitrocarburizing of low-carbon unalloyed steel

Part 1 *Mechanical properties*

S. DANNEFAER*, E. DREYER
Danfoss, Building L7, DK-6430 Nordborg, Denmark

Low-carbon unalloyed steel has been investigated after nitriding accomplished by either the salt-bath method (Tenifer) or the gas method (Nitroc). The resulting changes in the mechanical properties are reported in this paper, while changes in positron annihilation parameters are reported in Part 2. The mechanical properties show that the increase in both the lower yield stress and the ultimate stress is influenced greatly by the cooling rate after nitriding. A rapid cooling rate resulted in an increase of ~ 200 MPa while an increase of only 55 Mpa was observed for a slow cooling rate. These increases proved independent of prior straining in the range 0 to 20%, showing that the nitrogen uptake is not significantly influenced by internal defects. Annealing of rapidly cooled nitrided specimens resulted in a maximum of both the lower yield stress and the ultimate yield stress around 100° C. A transition from brittle to ductile fracture around this temperature was also observed. A large recovery of elongation to fracture was obtained after annealing at 140° C, which was not accompanied by any significant decrease in the lower yield stress. Dilatometer measurements indicated two precipitation stages, one around room temperature and another around 100° C.

1. Introduction

The process of nitriding steel has been employed in industry for many years, giving rise to a vast body of literature which deals with many different technological aspects (see [1] and references contained therein). More scientifically oriented investigations are much less numerous, but they do establish a fairly consistent picture of the basic processes which occur during nitriding [2–5].

During the nitriding process (which can be accomplished in many different ways) one can form a surface layer which consists of various iron nitrides. This surface layer is generally rather thin (5 to 20 μm) and very hard, around 1000 Vickers hardness, and has a crystal structure different from that of the original steel. Below this surface layer there exists another layer, the diffusion zone, into which nitrogen has diffused. No large scale phase transitions have occurred here, but one usually finds a certain amount of iron nitride precipitation which extends several hundred micrometres into the specimen. The nitrogen content is high in the surface layer but decreases rapidly near the interface between the surface layer and the diffusion zone to a rather low value, as recently shown by Auger spectroscopy [6, 7]. Usually the nitrogen content in the surface layer is about 6 to 10 wt% (22 to 37 at%) while that in the diffusion zone decreases from approximately 1 at% to zero with increasing depth from the interface.

Two main methods for nitrocarburizing are currently in use. The first method is a salt-bath type, where a molten salt-bath is the source of the nitrogen. The specimens are immersed in the molten bath, and then cooled at a fairly rapid rate at the end of the process by transferring them directly into brine or oil. The second method is gas nitriding in which the specimens are heated in a retort

*Present address: Department of Physics, University of Winnipeg, Winnipeg, Manitoba, Canada, R3B 2E9.

0022–2461/84 $03.00 + .12

TABLE I Analysis of the tensile bars

	C	Si	Mn	P	S	Fe
wt%	<0.1	<0.2	0.2–0.5	<0.045	<0.045	balance
at%	<1	<0.4	0.4–1.0	<0.08	<0.08	balance

containing a mixture of ammonia and various other gases, such as carbon dioxide. It is generally not possible to achieve rapid cooling at the end of this process since the specimens are inside the retort. Both of these processes are usually done at a temperature of between 550 and 580°C, so chosen to avoid the phase transition between α (ferrite) and γ (austenite) iron at 590°C in the iron–nitrogen phase diagram. It should be mentioned that there are several commercial processes available for nitriding such as plasma-nitriding, powder-nitriding and ion-implantation, each having its own peculiarities with respect to temperature, chemical composition and so on.

In the present investigations, nitrocarburizing achieved by the salt-bath method and the gas method have been investigated. These investigations were divided into two parts and are presented in this paper (Part 1) and the following paper (Part 2). The mechanical properties, principally the stress–strain relationships and hardness profiles, are presented in Part 1, while positron annihilation studies, which are capable of yielding information on defect structures at an atomic level, are presented in Part 2.

The present paper focuses on the influence on the mechanical properties of various degrees of deformation prior to the nitrocarburizing and on the effect of ageing of salt-bath-treated specimens. In particular, it was of interest to see if the positron results had some connection with the mechanical properties and if some new information could be obtained by this new method.

In Part 2 we then examine correlations between the mechanical properties and the information obtained in the positron annihilation studies in an attempt to discover the physical reasons for the changes in mechanical properties. Realizing that the results could have practical implications, commercial materials and nitrocarburizing processes were employed. The salt-bath and gas nitriding methods used were the commercial processes called Tenifer and Nitroc respectively.

2. Experimental details

Standard tensile bars (thickness 1 mm, width 12 mm) were cut from a deep-drawing material with the following analysis given in Table I. The surfaces of the tensile bars were in the as-received state, i.e. no polishing was done since the materials are not polished in practical use. Before nitriding, the tensile bars were divided into four groups. The first group received 0% tensile deformation, the second group 1.3%, the third 5% and the fourth group 20%. Each of these groups was again subdivided into two groups. One group was nitrided while the other received only the same thermal treatment as the nitrided group. This last group hence serves as a reference for the nitrided bars.

The salt-bath nitriding (Tenifer) was performed in a commercial bath for 1 h at 570°C, and the bars were rapidly cooled in brine at room temperature. The gas nitriding (Nitroc) was performed in a mixture of 95% dry HN_3 and 5% dry CO_2 at 570°C. The temperature patterns for these two processes are shown in Fig. 1 (the same patterns apply to the reference bars as mentioned above). All bars were stored at −35°C after their treatment in order to prevent ageing at room temperature.

3. Results

The stress–strain measurements for the various tensile bars were always repeated on four

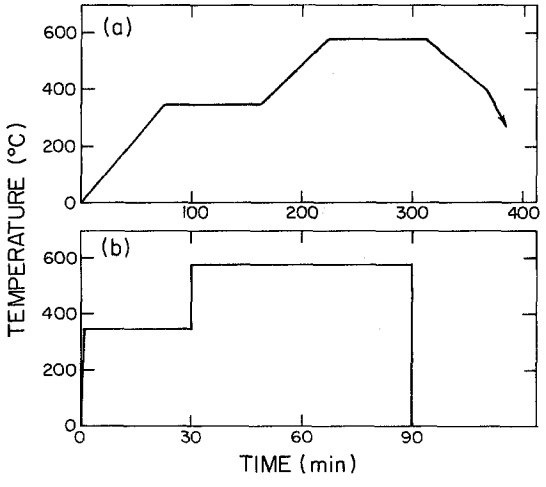

Figure 1 Temperature diagrams for (a) Nitroc treatment and (b) Tenifer treatment.

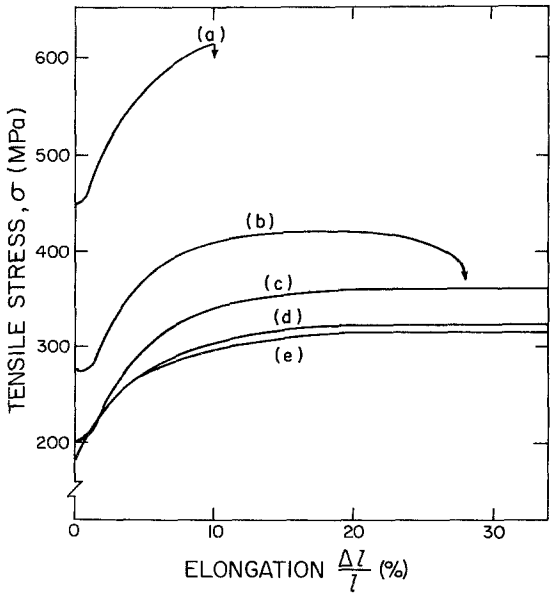

Figure 2 Stress–strain curves corresponding to various treatments of tensile samples. (a) Tenifer treated, (b) Nitroc treated, (c) reference specimen given same heat treatment as in Tenifer process, (d) reference specimen given same heat treatment as in Nitroc process, (e) as-received specimen. The arrows signify fracture.

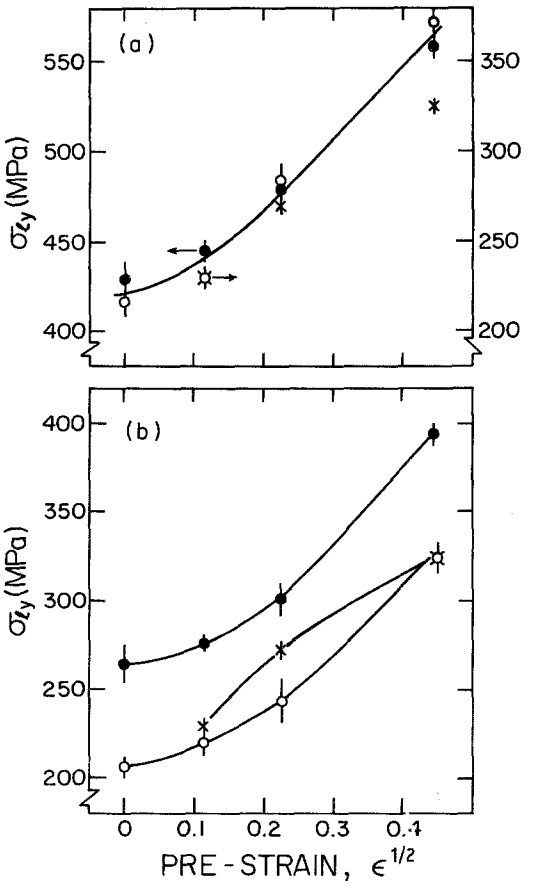

Figure 3 Lower yield stress, σ_{ly}, as a function of pre-strain for (a) Tenifer and (b) Nitroc treatments. The closed circles refer to the Tenifer- or Nitroc-treated bars, the open circles to the reference bars and the crosses indicate the stress at the pre-strain value prior to the treatments. Note that in the upper figure, the right-hand scale applies to the open circles and crosses, and that this scale is displaced by 200 MPa relative to the left-hand scale.

identically treated bars, and values reported are therefore the averages of the values obtained from the individual tests. For the sake of completeness actual average stress–strain curves are shown in Fig. 2 for tensile bars which were not subjected to any prior deformation. The heat treatments by themselves evidently result in a marginally stronger material, while the nitriding brings about a substantial increase in strength, especially for the Tenifer-treated samples. The treatments also result in a more or less well-defined lower yield point, σ_{ly}.

Similar curves were obtained for tensile bars which were subjected to various degrees of pre-straining before the heat treatments, and in Figs. 3 to 5 data for σ_{ly}, σ_{UTS} (ultimate tensile stress) and elongation to fracture, A, are collected. The reason for choosing for the abscissa the square root of the strain, ϵ, rather than ϵ itself, is that the dislocation density is roughly proportional to $\epsilon^{1/2}$ [8].

The salient features of Figs. 3 to 5 are as follows. Fig. 3 shows that the increase in σ_{ly} upon nitriding is nearly independent of the pre-strain value, the increase being about 200 MPa for the Tenifer-treated samples and 55 MPa for the Nitroc-treated samples. Note that the σ_{ly} value for the reference samples (i.e. heat-treated but not nitrided) corresponds rather closely to the stress value attained during the pre-straining. In other words, the heat-treatment itself does not anneal out any substantial amount of dislocations introduced by the pre-straining. As shown in Figs. 4 and 5, the increase in σ_{UTS} is again roughly constant at about 220 MPa for the Tenifer-treated samples, and approximately 55 MPa for the Nitroc-treated samples. The elongation, to fracture, A, is reduced for both treatments, but most markedly for the Tenifer-treated samples. It should be noted here that scanning electron microscopy showed that Nitroc-treated samples exhibited a ductile fracture in contrast to the brittle fracture for the Tenifer-treated samples.

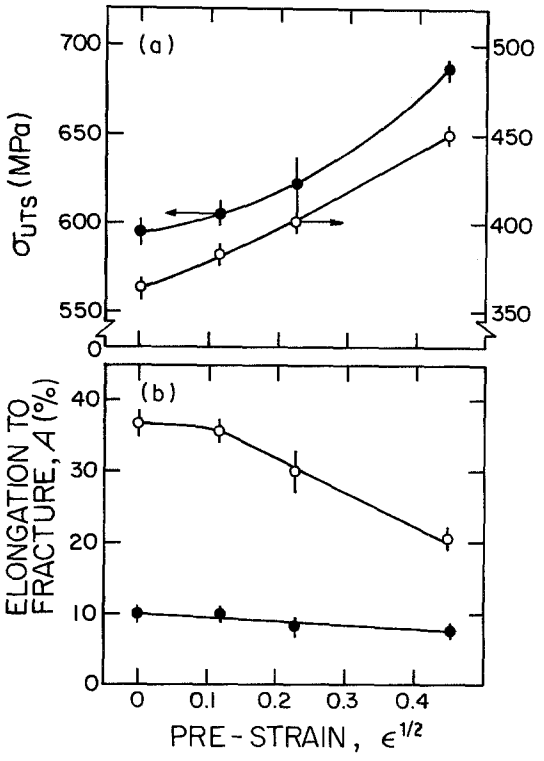

Figure 4 Ultimate tensile stress, σ_{UTS}, and elongation to fracture, A, as a function of pre-strain for Tenifer-treated samples (closed circles) and reference samples (open circles). Note that in the upper figure, the right-hand scale applies to the open circles, and that this scale is displaced by 200 MPa relative to the left-hand scale.

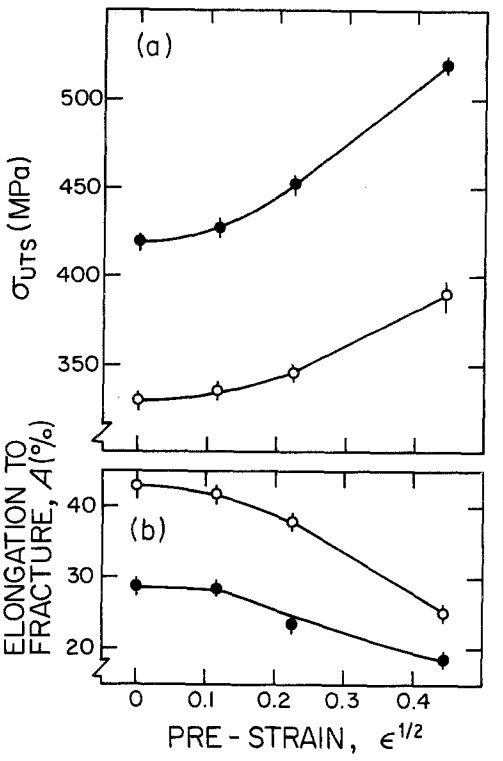

Figure 5 Ultimate tensile stress, σ_{UTS}, and elongation to fracture, A, as a function of pre-strain for Nitroc-treated samples (closed circles) and reference samples (open circles).

In order to obtain at least a qualitative idea as to the distribution of the nitrogen in the samples, metallurgical investigations were carried out. These investigations showed that the surface layers after both the Tenifer and Nitroc treatments had a thickness of $10 \pm 2\,\mu m$, and X-ray diffraction showed that this surface layer consisted of $Fe_{2-3}N$. No Fe_4N could be detected in the surface layer. The hardness profiles (hardness as a function of depth below the surface) are shown in Figs. 6 and 7. The hardness of the surface layer was measured to be about 1000 HV 0.05 (Vickers hardness using 50 g load). The hardness of the reference bars was measured for all four degrees of pre-strain and the values clustered inside the bands indicated in Figs. 6 and 7. For the Tenifer-treated bars, the hardness values for the 0%, 1.3%, and 5% pre-strains all seem to define one common curve which decreases towards the value obtained for the reference bars. The 20% pre-strained tensile bar, however, has much higher hardness values and does not, even in the centre of the tensile bar, attain the hardness of the reference bars. The hardness profiles for the Nitroc-treated bars exhibit a much less pronounced variation with depth, but interestingly the hardness does not decrease to the value obtained for the reference bars.

Since ageing at room temperature or at high temperatures is often utilized in industry, especially for Tenifer-treated samples, it was decided to investigate the Tenifer-treated tensile bars for different amounts of annealing. Annealing temperatures ranged from room temperature to 300° C with an annealing time of one hour. It should be stressed that this annealing is not the usual isochronal annealing. In the isochronal annealing scheme the *same* sample is annealed for a fixed time at ever increasing temperatures. In the present experiments a set of four bars (to facilitate repetitive tensile tests) was annealed at, say, 100° C for one hour, while another set was annealed at, say, 130° C and so on.

In Fig. 8 are shown the results of the tensile tests, as parametrized by σ_{UTS}, σ_{ly}, and A, for 0%

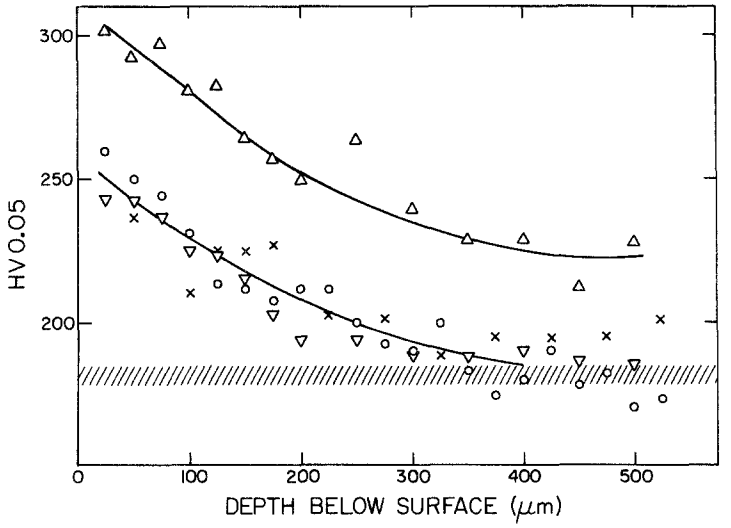

Figure 6 Vickers hardness (0.05 kg load) as a function of depth below the surface for Tenifer-treated samples. ○ 0% prestrain; × 1.3% pre-strain; ▽ 5% pre-strain; △ 20% pre-strain. The shaded horizontal band indicates the range of hardness values for the reference samples.

pre-strained tensile bars. The annealing curves show that both σ_{UTS} and σ_{ly} increase slightly with annealing temperature up to about 100° C and then rapidly decrease. The curve for the elongation to fracture, A, has essentially opposite behaviour, although not exactly a "mirror" image of the curves for σ_{ly} or σ_{UTS}. For the sake of comparison, it should be mentioned that the results for unaged Nitroc-treated tensile bars are in good agreement with 300° C aged Tenifer-treated tensile bars (compare Fig. 8 with Figs. 3 and 5).

A series of micrographs for the Tenifer-treated annealed bars and non-annealed Nitroc-treated bars are shown in Figs. 9 to 13. The first three micrographs illustrate the coarsening of the precipitates in the diffusion zone with increasing temperature. These pictures show a cross-section of the tensile bars, the surface layer being the relatively uniform band near the top of the photograph. Apparently the layer in Fig. 9 is cracked, but this is due to the technique used in preparing the sample for the micrograph. In this case an epoxy was utilized, and the brittle surface layer is apparently not adequately supported during polishing. Better results are shown in Figs. 10 and 11 where the samples were pressed against a soft copper plate. The diffusion zone is observable by virtue of the black etching precipitates. It is noteworthy that a change in the precipitation pattern could be unambiguously discerned only after the annealing at 200° C. At this stage, the micrograph shows a tendency towards the formation of elongated platelets which then coarsen substantially upon annealing at 300° C. Figs. 12 and 13 show micrographs for a gas nitrided sample which have an appearance suggesting a large amount of annealing.

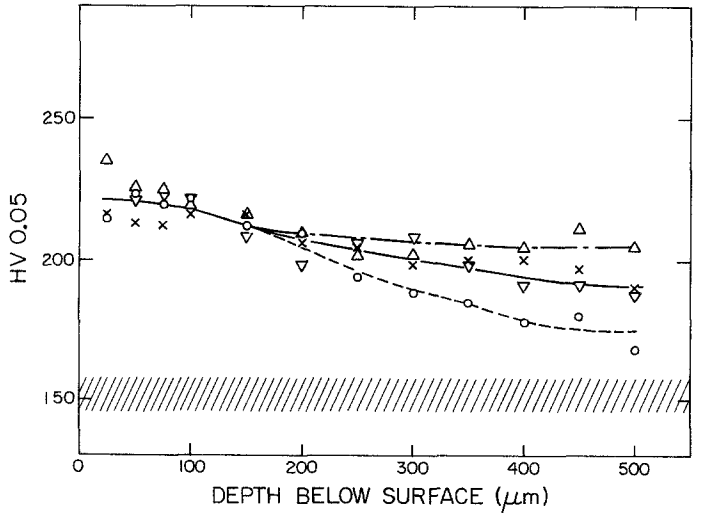

Figure 7 Vickers hardness (0.05 kg load) as a function of depth below the surface for Nitroc-treated samples. ○ 0% pre-strain; × 1.3% pre-strain; ▽ 5.0% pre-strain; △ 20% pre-strain. The shaded horizontal band indicates the range of hardness values for the reference samples.

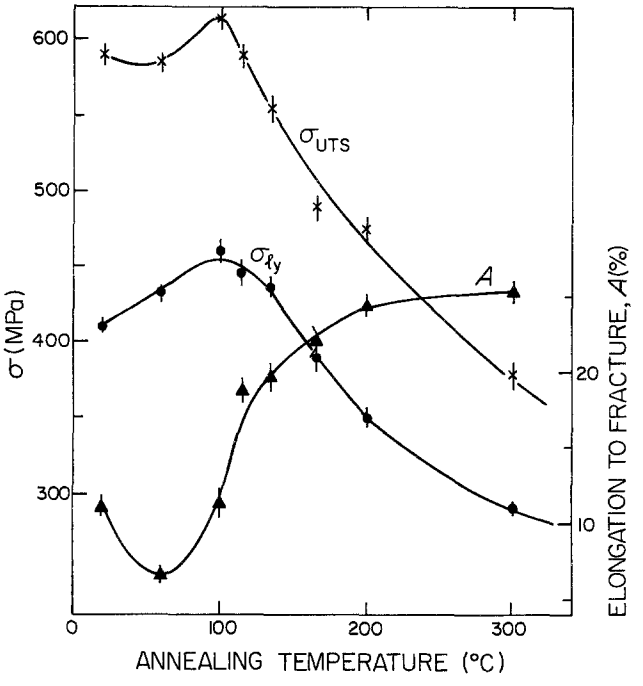

Figure 8 The dependence of σ_{UTS}, σ_{ly} and A on annealing temperature for Tenifer-treated samples with 0% pre-strain.

4. Discussion

The equilibrium phase diagram for the iron–nitrogen system is shown in Fig. 14. At the nitriding temperature (570 to 580° C), it is evident that no phase transition will take place between the α and γ phases (i.e. between iron having the bcc and the fcc crystal structures). The amount of nitrogen which can be dissolved at this temperature is at most ~0.4 at%. Two more phases may be present, depending on the nitrogen concentration, namely Fe_4N in the γ' and Fe_xN ($2 \lesssim x \lesssim 3$) in the so-called ϵ phase. During the cool-down from the nitriding temperature, the nitrogen in solid solution should decrease and eventually form the γ' phase. If the nitrogen content is less than about 26 at%, the ϵ phase could also transform in part to the γ' phase. As mentioned earlier, X-ray diffraction showed that the surface layer did not contain any Fe_4N, indicating that the nitrogen content here was above ~26 at%. This was the case for both Tenifer- and Nitroc-treated samples.

The precipitation of nitrogen from the solid solution is complex and depends of course on the cooling rate after the actual nitriding is finished.

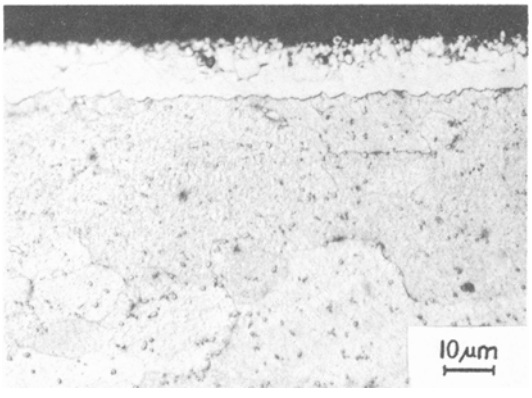

Figure 9 Micrograph of a Tenifer-treated sample aged at room temperature. The surface layer is the distinct band near the top of the photograph. Annealing up to 165° C did not result in any visible changes.

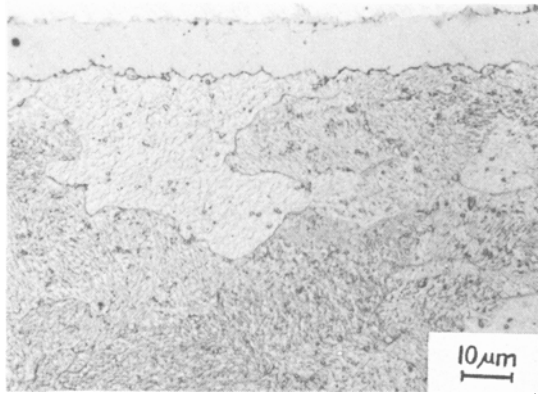

Figure 10 Micrograph of a Tenifer-treated sample annealed at 200° C for one hour. A slight coarsening of precipitates is evident.

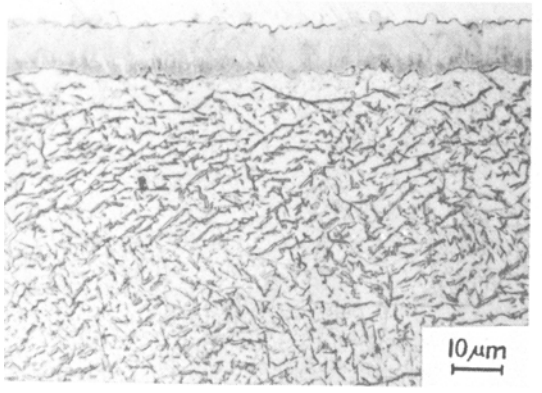

Figure 11 Micrograph of a Tenifer-treated sample annealed at 300° C for one hour. A very distinct coarsening of precipitates has taken place.

It has been shown [2] that the precipitation follows the route

$$\alpha\text{-Fe(N)} \rightarrow Fe_{16}N_2 \rightarrow Fe_4N$$

where α-Fe(N) denotes N dissolved in α-Fe. The intermediate phase, $Fe_{16}N_2$, is actually metastable, transforming above ~120° C to the stable Fe_4N phase. Since the Tenifer-treated samples are cooled much faster than the Nitroc-treated samples, it is only to be expected that the precipitation is much finer in the former case. The needle-like structure in the Nitroc-treated samples indicates acutally the formation of Fe_4N, while the apparent absence of this structure in the Tenifer-treated samples indicates predominantly $Fe_{16}N_2$. It is thus clear that even though both processes of nitriding may yield the same surface layer, the diffusion zone will certainly differ because of the different cooling rates.

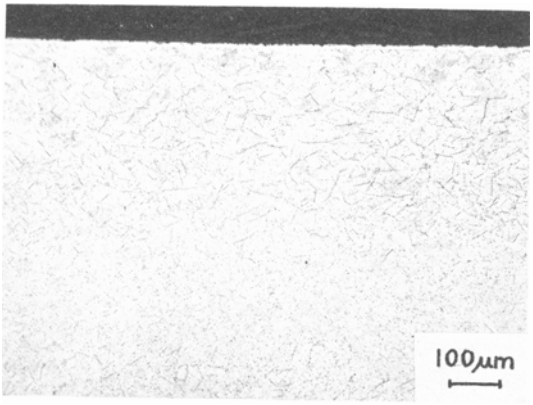

Figure 12 Micrograph of an unannealed Nitroc-treated sample showing the needle-like precipitation of Fe_4N.

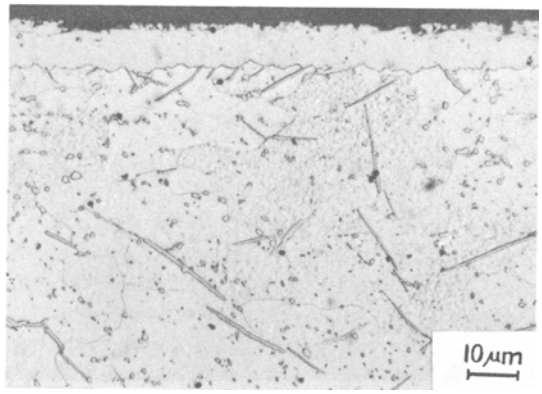

Figure 13 Same as Fig. 12 but with greater magnification.

4.1. The σ_{ly} and σ_{UTS} results

In general, precipitation will result in an increase in both the yield stress and the ultimate tensile stress due to the introduction of obstructions to the free movement of dislocations. One may imagine two extreme cases for the precipitation, one being the formation of a "cloud" of nitrogen atoms around the dislocations, the so-called Cottrell atmosphere, and the other being simply a formation of more or less coherent particles of Fe_xN. If the Cottrell atmosphere were the predominant mechanism, an increase in σ_{ly} independent of the pre-strain level would result, as is indeed observed (see Fig. 3). However, this mechanism would also imply a marked difference in the upper yield stress and the lower yield stress signifying the breaking away of dislocations from their associated Cottrell atmosphere. Such an effect was not observed, but it should be borne in mind that the size of this effect can often be influenced greatly by the testing machine itself. More importantly, a further consequence of this precipitation mechanism is that the *new* dislocations created after the yield point will not be associated with a

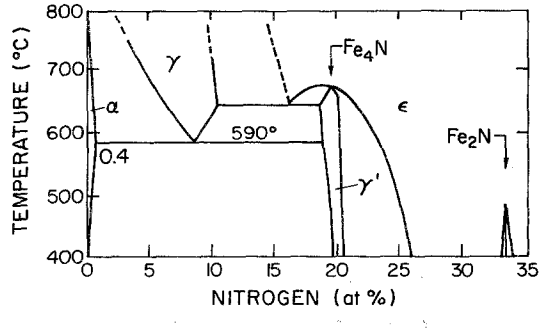

Figure 14 Iron–nitrogen equilibrium phase diagram.

Cottrell atmosphere, and consequently the increase in σ_{UTS} observed upon nitriding would be expected to be smaller than that for σ_{ly}. Comparing data for both Tenifer- and Nitroc-treated test bars show that the opposite is actually the case. We are therefore led to discard the Cottrell atmosphere mechanism as the only source for the strength increase.

The other extreme precipitation mechanism, that of particle formation, would increase σ_{ly} without any significant difference between upper yield stress and lower yield stress. It would also predict an increase in σ_{UTS} which is at least as large as that for σ_{ly}. Furthermore, the increases would be essentially independent of the pre-strain levels. It follows therefore that the stress–strain data point towards a precipitation of particles as the dominant strength-increasing mechanism. We note further than the increases for the Tenifer-treated bars are much greater than those for the Nitroc-treated bars. This would be expected due to the finer and more numerous precipitation in the former case (compare Figs. 9 and 13).

From a technological point of view, it should be mentioned that a rapid quenching brings about a substantial increase in σ_{ly} even in an unalloyed low-carbon steel. Generally this means that a higher load can be applied to a part without risk of cracking the brittle surface layer. The main difference between the Tenifer and Nitroc treatments thus stems from the difference in cooling rates rather than an actual difference in the nitriding processes.

4.2. Hardness measurements

The hardness profiles of Tenifer-treated bars which are shown in Fig. 6 can be analysed in terms of exponentially decreasing functions. For the three smallest degrees of tensile deformation (0, 1.3 and 5%) the expression is:

$$HV_{0.05} = 180 + 80\exp(-5.6x),$$

where $0 \leqslant x \leqslant d/2$ is the distance from the surface and d is the thickness ($\sim$ 1 mm) of the tensile bars. For the highest deformation degree (20%) the expression is:

$$HV_{0.05} = 180 + 128\exp(-4.4x) \times\{1 + \exp[4.4(2x - d/2)]\}.$$

The extra term in the curly bracket arises from the fact that the two profiles from each side of the tensile bar overlap each other. Evidently the increased defect density has increased the diffusion of nitrogen rather markedly.

This exponential behaviour is contrasted by the rather flat hardness curves for the Nitroc-treated tensile bars (see Fig. 7), which undoubtedly is due to the much more advanced degree of precipitation. This illustrates again the importance of the cooling rate. The fact that the hardness in the centre of all the tensile bars is higher than that for the reference bars indicates that the nitrogen has diffused a larger distance. This is undoubtedly a result of the longer time spent at higher temperatures (cf. Fig. 1).

It is of interest to compare the average hardness with the true stress, σ_T, at the point of fracture of the tensile bar. True stress refers to the (uniaxial) stress calculated from the load divided by the area of the fractured surface. The results for the treated and reference bars for the various pre-strain values are shown in Table II. It is quite clear that the Nitroc-treated tensile bars have nearly the same true stress at the point of fracture as the reference bars, an expected result due to the coarseness of the precipitates. The Tenifer-treated tensile bars have, again as expected, a much higher value of σ_T. For all cases, however, the usual value of the ratio $H/\sigma_T \approx 0.35$ is observed, even though average values of H were utilized. Nitriding thus does not significantly change the value of this empirically employed ratio.

4.3. Internal stresses

A commonly held view is that internal stresses resulting from nitriding could influence the mechanical properties of the material, particularly its resistance to fatigue. In the present investigations, therefore, the macroscopic stress in Tenifer-

TABLE II Comparison of true stress and average hardness to true stress ratio for Nitroc-treated, Tenifer-treated and reference specimens. ϵ, pre-strain value; σ_T, true stress; $\bar{H}$, average hardness

Treatment	ϵ (%)	σ_T (MPa)	$\sigma_T$ref (MPa)	$\bar{H}/\sigma_T$	$\overline{Href}/\sigma_T$ref
Nitroc	0	497	530	0.40	0.29
	1.3	495	529	0.41	0.29
	5	490	494	0.41	0.31
	20	531	462	0.40	0.33
Tenifer	0	661	461	0.31	0.39
	1.3	672	449	0.30	0.41
	5	674	423	0.30	0.43
	20	739	417	0.34	0.44

treated tensile bars was investigated using X-ray diffraction utilizing Co$K\alpha$ radiation. The surface layer was not removed since its removal would probably have modified the original stress distribution beneath the surface. The weak X-ray signal from the underlying α-iron showed no particular dependence on orientation or pre-strain value and yielded on average value of -14 ± 50 MPa for the internal stress. This indicates that the macroscopic stress introduced by the nitriding itself is very small indeed and would not have any practical significance.

Many measurements have been made of the stress levels resulting from nitriding [9, 10] and it has been argued that the increased resistance to fatigue is associated primarily with the formation of compressive stresses in the diffusion layer. In our opinion, however, the situation is more complex than this argument would indicate. When the surface layer is first created, a substantial change in its volume results, which can easily be calculated from the lattice parameters of α-iron and $Fe_{2-3}N$. In α-iron (bcc) the number of iron atoms is $8.50 \times 10^{22}\,cm^{-3}$, while in $Fe_{2-3}N$ (hcp structure [11]) the number of iron atoms ranges from 6.81 to $7.20 \times 10^{22}\,cm^{-3}$. Since the total number of iron atoms is conserved, the change in volume must range from 25% to 18%. Compressive stresses will therefore be established in the surface layer which tend to establish tensile stresses in the diffusion layer below. At the same time, the introduction of nitrogen into the diffusion layer will, by itself, tend to establish compressive stresses. This tendency toward compressive stresses would be small since, according to Mittemeijer *et al.* [12], the expansion in the diffusion zone in the absence of the influence of the surface layer would be at most 0.2%. Thus, it is certainly possible that the upper region of the diffusion zone is in a state of tension, while the lower region is in a state of compression.

4.4. Annealing results

As seen in Fig. 8, both σ_{ly} and σ_{UTS} have essentially the same dependence on annealing temperature. This result is anticipated in veiw of the earlier argument that precipitation is the dominant strength increasing mechanism, i.e. as the character of the precipitate changes with annealing, both σ_{ly} and σ_{UTS} would be expected to respond in a similar fashion.

Before annealing, the precipitate is undoubtedly $Fe_{16}N_2$ [2], the concentration of which apparently increases during the early stages of annealing causing an increase σ_{ly} and σ_{UTS}. At higher temperatures, the inevitable coarsening and associated reduction in concentration of the particles lead to a reduction in σ_{ly} and σ_{UTS}. At these higher temperatures the precipitate has taken the form Fe_4N [2].

It is of technological interest to note that, through a judicious choice of annealing temperature ($\sim 140^\circ C$), it is possible to maintain a large value of σ_{ly} while at the same time having recovered a large value of elongation to fracture. Investigations of the fractured surfaces by scanning electron microscopy after the tensile tests showed that the tensile bars annealed at temperatures of $100^\circ C$ or lower had a brittle fracture while those annealed above $115^\circ C$ had a ductile fracture.

The early stages of precipitation, i.e. in the temperature range 20 to $150^\circ C$, were further investigated by measuring the dilation of a Tenifer-treated bar during continuous heating at $1^\circ C\,min^{-1}$ followed by cooling at the same rate. The dilation curve obtained upon heating showed some structure up to $120^\circ C$ and then became linear corresponding to normal thermal expansion. Upon cooling, the dilation curve was purely linear and had the same slope as the dilation curve from an untreated reference bar. The dilation curve obtained during the cooling of the treated bar therefore serves as a reference and allows the dilation behaviour to be described as

$$\Delta l(T) = l_-(T) - l_+(T)$$

where $l_-(T)$ and $l_+(T)$ are the lengths of the bar at temperature T as T is decreased and increased respectively. The resulting $\Delta l(T)$ shown in Fig. 15 is therefore the consequence of an irreversible precipitation which, because of the removal of dissolved nitrogen and precipitate coarsening, causes a contraction of the treated bar. There are clearly two stages, one at 20 to $40^\circ C$ and another at 80 to $120^\circ C$. Taken together with the discussion of Fig. 8, the behaviour between 20 and $40^\circ C$ relates to the room temperature ageing, i.e. the precipitation of nitrogen from the supersaturated solution. The behaviour in the 80 to $120^\circ C$ range (near the maxima for σ_{ly} and σ_{UTS}) would then signify the coarsening of the $Fe_{16}N_2$ particles which would further reduce the lattice strain.

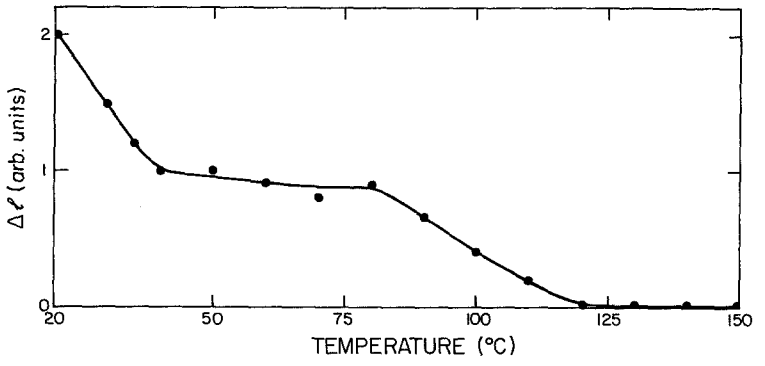

Figure 15 Irreversible dilation, Δl (see text), as a function of temperature for a 20% pre-strained Tenifer-treated sample.

5. Conclusion

This work on the mechanical properties of nitrided low-carbon unalloyed steel has shown the following:

1. Prior tensile deformation in the range 0% to 20% does not influence the effectiveness of the nitriding to any significant degree.

2. Changes in mechanical properties upon nitriding depend markedly on the rate of cooling following nitriding, with rapid cooling introducing the largest changes.

3. The internal macroscopic stress in both salt-bath and gas nitrided specimens is close to zero just below the surface layer.

4. Ageing of salt-bath nitrided specimens showed that most of the room temperature ageing took place within two hours as determined by the change in the lower yield stress. Annealing at higher temperatures showed a brittle-to-ductile transition of fracture at around 110° C and annealing at 300° C resulted in mechanical properties much like those for gas nitrided specimens.

5. A suitable choice of annealing temperature of salt-bath nitrided spceimens of around 140° C ensures a nearly complete retrieval of ductility without loss of the increases in yield and ultimate stress.

References

1. R. CHATTERJEE-FISCHER, *Härterei-Tech. Mitt* **36** (1981) 34, 91, 140, 205, 270, 335.
2. K. H. JACK, *Proc. Roy. Soc. London* **208A** (1951) 216.
3. N. DeCRISTOFARO and R. KAPLOW, *Met. Trans.* **8A** (1977) 425.
4. K. YAMAKAWA and F. E. FUJITA, *ibid.* **9A** (1978) 91.
5. D. GÉRARDIN, H. MICHEL, J. P. MORNIROLI and M. GANTOIS, *Mem. Sci. Rev. Met.* **74** (1977) 457.
6. C. DAWES, D. F. TRANTER and C. G. SMITH, *Metals Technol.* **6** (1979) 345.
7. P. F. COLIJN, W. H. KOOL, E. J. MITTEMEIJER and D. SCHALKOORD, *Sonderbände der Praktischen Metallographie* **12** (1981) 81.
8. S. MADER, A. SEEGER and H. M. THIERINGER, *J. Appl. Phys.* **34** (1963) 3376.
9. D. H. THOMAS and T. BELL, *Metal. Sci.* **14** (1980) 73.
10. E. J. MITTEMEIJER, A. B. P. VOGELS and P. J. van der SCHAAF, *Scripta Metall.* **14** (1980) 411.
11. K. H. JACK, *Acta Crystallogr.* **5** (1952) 404.
12. E. J. MITTEMEIJER, A. B. P. VOGELS and P. J. van der SCHAAF, *J. Mater. Sci.* **15** (1980) 3129.

Received 3 February
and accepted 24 June 1983